Organometallics **1986,** *5,* 2021–2030

Syntheses and Dynamic Stereochemistry of Hydrido–Carbonyl Heterobinuclear Metal–Metal Bonded Complexes. Crystal Structures of $MoPt(H)(\eta\text{-}C_5H_5)(CO)_3(PPh_3)_2(\mathit{Mo{-}Pt})$ and $MnPt(\mu\text{-}H)(\mu\text{-}CO)(CO)_4(PEt_3)_2(\mathit{Mn{-}Pt})$

Odile Bars,[1a,b] Pierre Braunstein,*[1b] Gregory L. Geoffroy,[1b,c] and Bernard Metz[1d]

Laboratoire de Chimie de Coordination, Associé au CNRS (UA 416), Université Louis Pasteur, 67070 Strasbourg Cédex, France, Laboratoire de Cristallochimie, Associé au CNRS (UA 254), Université de Rennes, 35042 Rennes Cédex, France, Department of Chemistry, The Pennsylvania State University, University Park, Pennsylvania 16802, and Laboratoire de Chimie Minérale ENSCS, Associé au CNRS (UA 405), Université Louis Pasteur, 67008 Strasbourg Cédex, France

Received October 30, 1985

The hydrido–carbonyl heterobinuclear complexes $MPt(H)(\eta\text{-}C_5H_5)(CO)_3(PPh_3)_2(\mathit{M{-}Pt})$ (M = Mo, **1**; M = W, **2**) and $MnPt(\mu\text{-}H)(\mu\text{-}CO)(CO)_4(PR_3)_2(\mathit{Mn{-}Pt})$ (R = Ph, **3**; R = Et, **4**) were prepared by the reaction of the corresponding carbonylmetalates with *trans*-$PtH(Cl)(PR_3)_2$. X-ray diffraction studies have been performed on complexes **1** and **4**. Data for **1**: monoclinic, $P2_1/n$, a = 15.42 (1) Å, b = 16.44 (1) Å, c = 16.50 (2) Å, β = 103.13 (5)°, V = 4076 Å^3, Z = 4, R = 0.053, R_w = 0.080 for 4159 reflections with $I \geq 3\sigma(I)$. The molecule consists of a $CpMo(CO)_3$ fragment bonded to a Pt atom (Mo–Pt = 2.839 (1) Å) which is further ligated by two mutually cis PPh_3 ligands and a hydride ligand in a terminal position. Data for **4**: monoclinic, $P2_1/n$, a = 11.142 (2) Å, b = 18.999 (4) Å, c = 11.661 (2) Å, β = 104.81 (1)°, V = 2387 Å^3, Z = 4, R = 0.059, R_w = 0.075 for 2899 reflections with $I \geq 3\sigma(I)$. The environment about the Pt atom is planar and consists of the two mutually cis PEt_3 ligands, the bridging carbonyl, and the bridging hydride (the latter not located by X-ray diffraction). The Mn atom, which is in the octahedral environment defined by the bridging ligands and the four terminal carbonyls, is at distance of 2.730 (2) Å from the Pt atom. Spectroscopic, IR, and ^1H, $^{31}P\{^1H\}$, and ^{31}P NMR data are discussed and are consistent with the structure of the complexes. These heterobinuclear complexes undergo a unique fluxional process, which is detailed for **1** and **4**. The observed changes in the temperature-dependent ^1H NMR spectra imply a mutual exchange process, equivalencing the phosphorus atoms, that maintains spin correlation and is thus strictly intramolecular and nondissociative, within the limits of the NMR experiment. The mechanism is discussed, and connections made with the chemical behavior of the complexes.

Introduction

The selective interaction of small molecules and organic ligands with heterometallic centers is a topic of wide current interest in organometallic cluster chemistry.[2] Mixed-metal clusters are ideally suited to coordinate various ligands in a unique manner,[3] allowing unusual chemical transformations to occur. This is especially true when the metals have widely different chemical properties as found in "early–late" complexes which combine metals from the groups 4–6 with those of group 8. Hydride ligands are particularly valuable components of such polynuclear complexes since they are known to facilitate many stoichiometric and catalytic reactions of organic substrates.

While a number of heteropolynuclear carbonyl complexes have been prepared in which group 6 and 7 metals have been combined with metals of the Ni triad, relatively few *heterobinuclear* complexes, the simplest members of the heteropolynuclear family, have been synthesized and studied.[3,4] Such complexes would be particularly valuable for studying the fundamental reactivity resulting from combinations of these particular metals. We have prepared a series of hydrido–carbonyl heterobinuclear complexes containing Mo, W, and Mn bonded to Pt and report here our results on the synthesis, stability, structure, and dynamic behavior of these complexes.[6]

Experimental Section

All experimental procedures were performed in standard Schlenk-type flasks under an atmosphere of purified nitrogen,[5] as detailed in previous papers from this laboratory.[7] All solvents were dried by refluxing under nitrogen with the appropriate drying agent and distilled just prior to use. Chromatography was performed under nitrogen, using a silica gel column (Kieselgel 60, Merck). The following compounds were prepared by literature procedures: *trans*-$PtH(Cl)(PEt_3)_2$,[8] *trans*-$PtH(Cl)(PPh_3)_2$,[9a] $Na[Mo(CO)_3Cp]\cdot 2DME$,[10] and $Na[W(CO)_3Cp]\cdot 2DME$.[10] Solutions of $Na[Mn(CO)_5]$ were prepared by Na/Hg reduction of $Mn_2(CO)_{10}$ in THF.[11] Elemental analyses (C, H, and P) were performed by the Service Central de Microanalyses du CNRS. Mass spectra were measured on a Thompson THN mass spectrometer (EI, 70 eV, 8 kV) by Dr. G. Teller (Université Louis Pasteur). IR spectra were recorded in the 4000–400 cm^{-1} region on a Perkin-Elmer 398 spectrophotometer as KBr pellets, unless otherwise specified. NMR spectra (^1H, ^{13}C, $^{31}P\{^1H\}$) were recorded on a FT-Bruker WH-90 or Cameca 250 instrument. Proton and carbon chemical shifts are positive downfield relative to external Me_4Si. Positive phosphorus chemical shifts indicate a downfield position relative to H_3PO_4. The reactions were generally monitored by IR in the ν(CO) region.

---

[1] (a) Université de Rennes. (b) Laboratoire de Chimie de Coordination, Strasbourg. (c) The Pennsylvania State University. (d) ENSCS, Strasbourg.

[2] Sappa, E.; Tiripicchio, A.; Braunstein, P. *Coord. Chem. Rev.* **1985,** *65,* 219.

[3] Roberts, D. A.; Geoffroy, G. L. In *Comprehensive Organometallic Chemistry*; Wilkinson, G., Stone, F. G. A., Abel, E. W., Eds.; Pergamon Press: Oxford, 1982; Chapter 40.

[4] Bruce, M. I. *J. Organomet. Chem.* **1985,** *283,* 339.

[5] Shriver, D. F. *The Manipulation of Air Sensitive Compounds*, McGraw-Hill: New York, 1969.

[6] Portions of this work have appeared as preliminary communications: (a) Bars, O.; Braunstein, P. *Angew. Chem., Int. Ed. Engl.* **1982,** *21,* 308. (b) Braunstein, P.; Geoffroy, G. L.; Metz, B. *Nouv. J. Chim.* **1985,** *9,* 221.

[7] Bender, R.; Braunstein, P.; Jud, J. M.; Dusausoy, Y. *Inorg. Chem.* **1984,** *23,* 4489.

[8] Parshall, G. W. *Inorg. Synth.* **1970,** *12,* 28.

[9] (a) Bailar, J. C.; Itatani, H. *Inorg. Chem.* **1965,** *4,* 1618. (b) Chatt, J.; Shaw, B. L. *J. Chem. Soc. A* **1962,** 5075. (c) Collamati, I.; Furlani, A.; Attioli, G. *J. Chem. Soc. A* **1970,** 1694.

[10] Bender, R.; Braunstein, P.; Jud, J. M.; Dusausoy, Y. *Inorg. Chem.* **1983,** *22,* 3394.

[11] Hieber, W.; Wagner, G. *Z. Naturforsch.* **1958,** *B13,* 339.

0276-7333/86/2305-2021$01.50/0 © 1986 American Chemical Society

Synthesis of *cis*-MoPt(H)Cp(CO)$_3$(PPh$_3$)$_2$ (1). 1. A tetrahydrofuran (THF) solution (50 mL) of Na[Mo(CO)$_3$Cp]·2DME (1.121 g, 2.50 mmol) was added to a suspension of *trans*-PtH(Cl)(PPh$_3$)$_2$ (1.890 g, 2.50 mmol) in THF (20 mL) at -40 °C. The reaction temperature was slowly raised to 0 °C, and the solution turned red. The reaction mixture was stirred for 1 h at 0 °C and then filtered to remove NaCl. An equal volume of pentane was added to this solution, and after the solution was cooled to -20 °C, an orange powder precipitated which was recrystallized from toluene/pentane, affording orange, air-stable (for at least 1 week) crystals of *cis*-MoPt(H)Cp(CO)$_3$(PPh$_3$)$_2$ (1; 1.00 g, 41.4% based on Pt) (mp 158 °C): IR ν(PtH) 2108 (m) cm^{-1}, ν(CO) 1919 (s), 1831 (s), 1803 (s) cm^{-1}, ν(CO) (THF) 1928 (vs), 1836 (s), 1820 (s) cm^{-1}; ^{1}H NMR (toluene-d_8, -40 °C) δ -5.73 (d, 1 H, PtH, $|^2J(\mathrm{PH})|$ = 170 Hz, $^1J(\mathrm{PtH})$ = 678 Hz), 5.44 (s, 5 H, Cp); ^{31}P{^{1}H} NMR (THF/C$_6$D$_{12}$, -45 °C) δ 31.9 (d, P(1), $^2J(\mathrm{PP})$ = 6 Hz, $^1J(\mathrm{PtP})$ = 3690 Hz), 35.5 (d, P(2), $^1J(\mathrm{PtP})$ = 2653 Hz); MS, *m/e* (EI) 862 (M$^+$ - CO - C$_6$H$_5$ + 2H$^+$), 797 (M$^+$ - CO - C$_6$H$_5$ - C$_5$H$_5$ + 2 H$^+$), 720 (M$^+$ - CO - 2C$_6$H$_5$ - C$_5$H$_5$ + 2H$^+$). Anal. Calcd for C$_{44}$H$_{36}$MoO$_3$P$_2$Pt (fw 965.75): C, 54.72; H, 3.76; P, 6.41. Found: C, 54.82; H, 3.61; P, 6.28.

2. To test the effect of temperature, this reaction was repeated at room temperature. After filtration of the reaction mixture, successive precipitation of the products was achieved by addition of increasing amounts of pentane and cooling of the solution. Thus, we isolated orange crystals of 1 (0.578 g, 24%), black crystals of Pt$_4$(μ-CO)$_5$(PPh$_3$)$_4$ (0.073 g, 6%) identified by comparison with an authentic sample,[12] red crystals of the known[13] Pt$_5$(μ-CO)$_5$(CO)(PPh$_3$)$_4$ (0.046 g, 4.2%), and Ph$_3$P=O (0.096 g).

3. Purification of the desired complex by chromatography was also attempted, but this led to undesired but interesting chemical transformations. For example, the reaction described under 1 was repeated on a larger scale, starting from *trans*-PtH(Cl)(PPh$_3$)$_2$ (3.02 g, 4 mmol) and Na[Mo(CO)$_3$Cp]·2DME (1.793 g, 4 mmol). After filtration of the reaction mixture, the solution was impregnated onto silica gel and evaporated to dryness under vacuum. The impregnated silica gel was transferred onto a chromatography column loaded with silica gel and pentane. Elution with a 100:40 pentane/toluene mixture afforded [Mo(CO)$_3$Cp]$_2$ (0.112 g, 11.4%). At this point, it was noted that the orange color of the impregnated silica gel, attributed to the presence of 1 (cf. 1 and 2) had been replaced by a black color, indicating that decomposition of the heterobimetallic complex had occurred as soon as product migration had started. Elution with toluene afforded a red solution of Pt$_5$(μ-CO)$_5$(CO)(PPh$_3$)$_4$[13] (0.110 g, 6.3%), and further elution with a 100:20 toluene/THF mixture afforded white *trans*-PtH(Cl)(PPh$_3$)$_2$ (0.345 g, 11.4%) and green-black Pt$_2$Mo$_2$Cp$_2$(CO)$_6$(PPh$_3$)$_2$[7] (ca. 0.15g, 5.3%), which were separated by fractional crystallization. Elution with THF gave a PPh$_3$-containing platinum complex (0.120 g), presenting a strong IR absorption at 1680 cm^{-1}, and some Pt(PPh$_3$)$_3$ (0.015 g, 0.4%). Finally, elution with acetic acid (CH$_3$COOH (100%)/H$_2$O, 1:2) afforded a platinum acetato complex (0.40 g) which could be converted into Pt(PPh$_3$)$_2$Cl$_2$ by reaction with LiCl.

Synthesis of WPt(H)Cp(CO)$_3$(PPh$_3$)$_2$ (2). The procedure used was similar to that described above for the synthesis of 1 under procedure 1, replacing Na[Mo(CO)$_3$Cp]·2DME with Na[W(CO)$_3$Cp]·2DME. When the reaction mixture was precipitated with pentane at 0 °C, an orange powder was obtained with IR [ν(PtH) 2116 (m) cm^{-1}, ν(CO) 1917 (vs), 1828 (vs), 1808 (vs) cm^{-1}, ν(CO)(THF) 1925 (vs), 1835 (m), 1815 (s) cm^{-1}], indicating the presence of WPt(H)Cp(CO)$_3$(PPh$_3$)$_2$ (2). Unfortunately, this compound was contaminated with some *trans*-PtH(Cl)(PPh$_3$)$_2$ [ν(PtH) 2220 (m) cm^{-1}] and could not be completely purified by fractional crystallization. Solutions of 2 slowly decomposed with formation of Pt$_4$(μ-CO)$_5$(PPh$_3$)$_4$[12] and unidentified tungsten-containing species. No [W(CO)$_3$Cp]$_2$ was detected by IR. Attempts at chromatographic separation also failed. With pentane, no product migration took place, and with toluene, decomposition of 2 occurred and Pt$_5$(μ-CO)$_5$(CO)(PPh$_3$)$_4$[13] was collected as a red fraction.

Synthesis of MnPt(H)(CO)$_5$(PPh$_3$)$_2$ (3). A THF solution (50 mL) of Na[Mn(CO)$_5$], prepared from Mn$_2$(CO)$_{10}$ (0.487 g, 1.25 mmol), was added to a suspension of *trans*-PtH(Cl)(PPh$_3$)$_2$ (1.89 g, 2.5 mmol) in THF (20 mL) at -60 °C. The temperature was maintained constant for 0.5 h. Cold pentane (150 mL) was then added to ensure complete precipitation of the orange reaction product. It was filtered, rapidly washed with deoxygenated water to remove NaCl, and dried in vacuo. No trace of *trans*-PtH(Cl)(PPh$_3$)$_2$ was found in this compound which was assigned the formula MnPt(H)(CO)$_5$(PPh$_3$)$_2$ (3; 1.35 g, 59%): IR ν(CO) 2049 (s), 1963 (vs, br), 1918 (vs), 1794 (m, br), 1723 (vs) cm^{-1}; MS, *m/e* (EI) 831 (M$^+$ - 3CO), 774 (M$^+$ - 5CO - H), 697 (M$^+$ - 5CO - H - C$_6$H$_5$). Anal. Calcd for C$_{41}$H$_{31}$MnO$_5$P$_2$Pt (fw 915.67): C, 53.73; H, 3.41. Found: C, 53.80; H, 3.52.

If the reaction mixture was instead allowed to slowly warm to room temperature and then stirred for 4 h until the IR spectrum indicated no further change, precipitation by addition of increasing amounts of pentane and cooling afforded successively black Pt$_4$(μ-CO)$_5$(PPh$_3$)$_4$[12] (0.139 g, 11.3%), yellow Pt$_2$Cl$_2$(μ-CO)(PPh$_3$)$_3$[14] (0.055 g, 3.4%), a beige powder (0.140 g) presenting infrared ν(CO) absorptions at 2020 (s) and 1910 (s, br) cm^{-1} and aromatic vibrations, red Pt$_3$(μ-CO)$_3$(PPh$_3$)$_4$[12] (0.037 g, 2.6%), and very small amounts of Mn$_2$(CO)$_{10}$, Mn$_2$(CO)$_9$PPh$_3$, and Mn$_2$(CO)$_8$(PPh$_3$)$_2$, characterized by their IR spectra.[15]

Synthesis of MnPt(μ-H)(μ-CO)(CO)$_4$(PEt$_3$)$_2$ (4). A THF solution of Na[Mn(CO)$_5$] (11 mL of a 0.039 M solution prepared by reacting 0.191 g of Mn$_2$(CO)$_{10}$ with Na/Hg in 25 mL of THF) was added to a solution of *trans*-PtH(Cl)(PEt$_3$)$_2$ (0.205 g, 0.44 mmol) in THF (50 mL) that had been precooled to -78 °C in a dry ice/acetone slush bath. The solution was stirred at -77 °C for 4 h during which time it changed from colorless to orange. The solvent was removed at 0 °C under vacuum to leave an orange-brown residue. It was extracted with three 25-mL portions of pentane to yield an orange pentane solution and a brown residue. The brown residue, partly soluble in toluene, was not otherwise characterized. Evaporation of solvent from the pentane extract gave orange-brown microcrystalline PtMn(μ-H)(μ-CO)(CO)$_4$(PEt$_3$)$_2$ (4; 0.154 g, 56% based on Pt) (mp 60-62 °C with decomposition under N$_2$ to an oily brown material): IR ν(CO) (KBr) 2040 (m), 1948 (vs), 1910 (vs), 1708 (s) cm^{-1}, ν(CO)(THF) 2040 (m), 1950 (vs), 1924 (s), 1720 (m) cm^{-1}, ν (CO) (hexane) 2056 (m), 1973 (m), 1963 (vs), 1941 (s), 1729 (m) cm^{-1}; ^{1}H NMR (toluene-d_8, -23 °C) δ -3.80 (dd, 1 H, Pt*H*, $|^2J(\mathrm{PH})|$ = 76.7, 29.2 Hz, $^1J(\mathrm{PtH})$ = 409 Hz); ^{31}P{^{1}H} NMR (C$_6$D$_6$, 18 °C) δ 5.69 (s, P(2), $^1J(\mathrm{PtP})$ = 2167 Hz), 29.15 (s, P(1), $^1J(\mathrm{PtP})$ = 4580 Hz). Anal. Calcd for C$_{17}$H$_{31}$O$_5$P$_2$MnPt (fw 627.41): C, 32.54; H, 4.98. Found: C, 32.03; H, 4.93.

X-ray Diffraction Studies of 1 and 4. Orange single crystals of 1 were grown by slow diffusion of pentane into a toluene solution of the complex at -20 °C. Orange single crystals of 4 were obtained by cooling a saturated pentane solution of the complex to -22 °C in a laboratory freezer. The structure of 1 was determined by O.B. and that of 4 by B.M. Diffraction data were collected on Enraf-Nonius four-circle CAD4 automated diffractometers. Cell constants and other pertinent data are collected in Table I. Data were corrected for Lorentz and polarization effects. For 1, data were also corrected for absorption. For 4, for which decomposition during data collection could not be prevented, even under argon at 0 °C, the data were corrected for decay (36% controlled by three standard reflections), not for absorption. The structures were solved by direct methods, using MULTAN,[16] which gave the location of the metal atoms. The remaining non-hydrogen atoms were located by successive difference Fourier maps. Calculations were performed on a PDP 11 computer with SDP system.[17] Anisotropic thermal parameters were assigned to all non-hydrogen atoms of 1 and 4. The hydrogen atoms of the phenyl and ethyl groups of 1 and 4, respectively, were introduced by their computed

---

[12] Chatt, J.; Chini, P. *J. Chem. Soc A* **1970**, 1538.

[13] Barbier, J. P.; Bender, R.; Braunstein, P.; Fischer, J.; Ricard, L. *J. Chem. Res., Synop.* **1978**, 230; *J. Chem. Res., Miniprint* **1978**, 2913.

[14] Bender, R.; Braunstein, P.; Tiripicchio, A.; Tiripicchio Camellini, M. *J. Chem. Soc., Chem. Commun.* **1984**, 42.

[15] Haines, L. I. B.; Hopgood, D.; Poë, A. J. *J. Chem. Soc. A* **1968**, 421.

[16] Germain, G.; Main, P.; Woolfson, M. M. *Acta Crystallogr., Sect. A: Cryst. Phys., Diffr., Theor. Gen. Crystallogr.* **1971**, *A27*, 368.

[17] Frenz, B. A. *The Enraf-Nonius CAD4-SDP*, In *Computing in Crystallography*; Schenk, H., Olthof-Hazekamp, R., van Koningsveld, H., Bassi, G. C., Eds.; University Press: Delft, The Netherlands, 1978; pp 64-71.

Table I. Summary of Crystal Data and Intensity Collection of 1 and 4

	$MoPt(H)Cp(CO)_3(PPh_3)_2$ (1)	$MnPt(\mu\text{-}H)(\mu\text{-}CO)(CO)_4(PEt_3)_2$ (4)
formula	$C_{44}H_{36}O_3P_2MoPt$	$C_{17}H_{31}O_5P_2MnPt$
fw	965.75	627.41
crystal system	monoclinic	monoclinic
space group	$P2_1/n$	$P2_1/n$
a, Å	15.42 (1)	11.142 (2)
b, Å	16.44 (1)	18.999 (4)
c, Å	16.50 (2)	11.661 (2)
β, deg	103.13 (5)	104.81 (1)
V, Å^3	4076	2387
Z	4	4
d(calcd), g cm^{-3}	1.57	1.75
cryst dimens, mm	0.2 × 0.2 × 0.18	0.12 × 0.18 × 0.24
F(000), e	1896	1224
temp, °C	25	0 (Lindemann glass capillary under argon)
diffractometer	Enraf-Nonius CAD4	Enraf-Nonius CAD 4
radiation (graphite monochromator)	Mo Kα (λ = 0.710730 Å)	Cu Kα (λ = 1.54184 Å)
linear abs coeff, cm^{-1}	40.28	167.49
scan type	$\omega-2\theta$	$\omega-2\theta$
scan range, deg	$1.0 + 0.35 \tan\theta$	$0.70 + 0.14 \tan\theta$
θ limits, deg	1–27	2–62
data collected	8297	3752
unique data used	4159 ($I \geq 3\sigma(I)$)	2899 ($I \geq 3\sigma(I)$)
$R = \sum(\lvert F_o\rvert - \lvert F_c\rvert)/\sum\lvert F_o\rvert$	5.3	5.9
$R_w = (\sum w(\lvert F_o\rvert - \lvert F_c\rvert)^2/\sum w\lvert F_o\rvert^2)^{1/2}$	8	7.5
std error in an observn of unit weight, e	1.75	1.60
P fudge factor	0.07	0.07

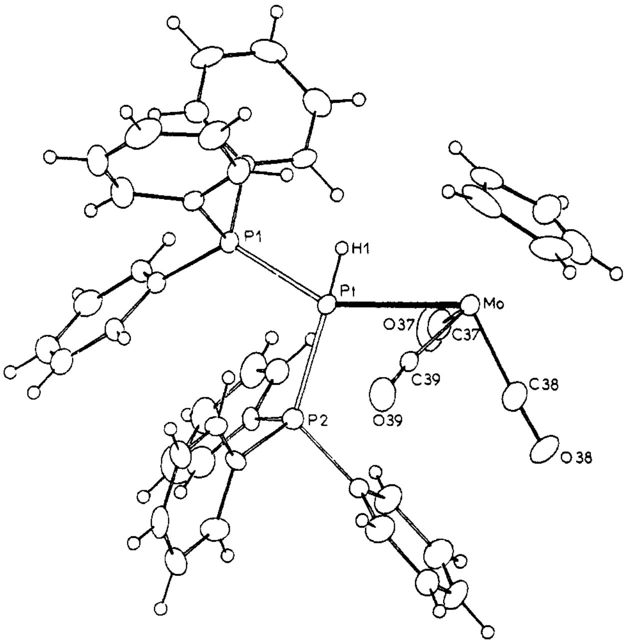

Figure 1. A view of the structure of $MoPt(H)(\eta\text{-}C_5H_5)(CO)_3(PPh_3)_2$ (1). The hydride ligand was placed at 1.6 Å from the Pt atom. A drawing showing the complete atom numbering scheme is given in the supplementary material.

coordinates in structure factor calculations and were assigned isotropic thermal parameters of $B = 5.0$ Å^2. The final full-matrix least-squares refinement led to the values of the residuals given in Table I, with $R = \sum(\lvert\lvert F_o - F_c\rvert\rvert)/\sum\lvert F_o\rvert$ and $R_w = [\sum w(\lvert F_o\rvert - \lvert F_c\rvert)^2/\sum w\lvert F_o\rvert^2]^{1/2}$, with $w = 1/\sigma^2(F_o)$. A final difference map for 4 showed peaks up to 1.33 eÅ^{-3} situated in the vicinity of the Pt atom, but none of them could be assigned with certainty. Final values of all refined atomic positional parameters (with esd's) are listed in Tables II and III, and relevant bond distances and angles (with esd's) are summarized in Tables IV and V, respectively. Tables of selected least-squares planes, thermal parameters, calculated hydrogen atom positions, and structure factors are given in the supplementary material.

Results

Preparation and Characterization of the Complexes. We have previously succeeded in preparing heterotrinuclear chain complexes m–PtL$_2$–m by the reaction of carbonylmetalates [m$^-$] (e.g., $CpMo(CO)_3^-$ or $Mn(CO)_5^-$) with platinum(II) dihalogeno complexes, as shown in eq 1.[7,18–20] We have now found that this synthetic approach

$$2Na[m] + trans\text{-}PtCl_2(PhCN)_2 \rightarrow m\text{–}Pt(PhCN)_2\text{–}m + 2NaCl \quad (1)$$

can be applied to platinum complexes containing a hydride and one chloride ligand instead of two chlorides. With only one leaving group on platinum, this reaction results in hydrido heterobinuclear complexes (eq 2 and 3).

$Na[M(CO)_3Cp] + trans\text{-}PtH(Cl)(PPh_3)_2 \rightarrow NaCl +$

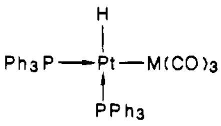

$$Ph_3P\text{—}\overset{\displaystyle H}{\underset{\displaystyle PPh_3}{Pt}}\text{—}M(CO)_3Cp \quad (2)$$

1, M = Mo
2, M = W

$Na[Mn(CO)_5] + trans\text{-}PtH(Cl)(PR_3)_2 \rightarrow NaCl +$

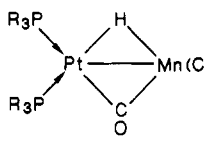

(3)

3, R = Ph
4, R = Et

The reactions in eq 2 were carried out at low or room temperature in THF, the best yields being obtained when working below 0 °C. Complex 2 in solution appeared to be more labile than 1 and was not isolated analytically pure. However, its spectroscopic data leave no doubt about its formulation and structure. The IR spectra of 1 and 2 showed absorptions at 2108 and 2116 cm^{-1}, respectively,

---

[18] Braunstein, P.; Dehand, J. *J. Organomet. Chem.* **1974**, *81*, 123; *Bull. Soc. Chim. Fr.* **1975**, 1997.

[19] Barbier, J. P.; Braunstein, P. *J. Chem. Res. Synop.* **1978**, 412; *J. Chem. Res., Miniprint* **1978**, 5029.

[20] Braunstein, P.; Keller, E.; Vahrenkamp, H. *J. Organomet. Chem.* **1979**, *165*, 233.

Table II. Atomic Coordinates for Non-Hydrogen Atoms and Equivalent Thermal Parameters[a] for $MoPt(H)Cp(CO)_3(PPh_3)_2$ (1)

atom	*x*	*y*	*z*	*B*(eqv),[b] Å^2
Pt	0.23420 (4)	0.06039 (4)	0.06270 (4)	2.49 (1)
Mo	0.1962 (1)	−0.08803 (8)	−0.02625 (8)	2.75 (3)
P(1)	0.2524 (3)	0.1296 (2)	0.1841 (2)	2.57 (8)
P(2)	0.2922 (3)	0.1537 (3)	−0.0196 (3)	2.74 (9)
O(37)	0.3983 (8)	−0.0468 (9)	0.0279 (10)	6.4 (4)
O(38)	0.2292 (8)	−0.0924 (9)	−0.2043 (7)	5.1 (3)
O(39)	0.0835 (8)	0.0599 (8)	−0.1019 (8)	5.0 (3)
C(1)	0.3127 (10)	0.2245 (9)	0.1992 (9)	2.6 (3)
C(2)	0.3993 (10)	0.2285 (10)	0.2438 (9)	3.1 (4)
C(3)	0.4470 (11)	0.2994 (12)	0.2529 (10)	4.3 (4)
C(4)	0.4046 (13)	0.3696 (12)	0.2156 (12)	5.6 (5)
C(5)	0.3165 (13)	0.3671 (11)	0.1706 (11)	4.3 (4)
C(6)	0.2719 (11)	0.2966 (9)	0.1622 (9)	3.2 (4)
C(7)	0.3130 (10)	0.0680 (9)	0.2721 (8)	2.9 (3)
C(8)	0.3186 (12)	0.0903 (11)	0.3545 (10)	4.0 (4)
C(9)	0.3634 (12)	0.0464 (13)	0.4172 (9)	4.6 (5)
C(10)	0.4071 (12)	−0.0249 (12)	0.4026 (11)	4.9 (4)
C(11)	0.4054 (12)	−0.0484 (11)	0.3227 (12)	4.4 (5)
C(12)	0.3592 (11)	−0.0013 (11)	0.2594 (9)	3.5 (4)
C(13)	0.1497 (9)	0.1525 (9)	0.2165 (9)	2.6 (3)
C(14)	0.0825 (11)	0.0930 (11)	0.2038 (10)	3.6 (4)
C(15)	0.0048 (11)	0.1049 (14)	0.2317 (11)	4.6 (5)
C(16)	−0.0054 (12)	0.1795 (14)	0.2696 (11)	6.0 (5)
C(17)	0.0597 (13)	0.2384 (11)	0.2846 (12)	5.2 (5)
C(18)	0.1355 (12)	0.2246 (11)	0.2596 (12)	4.6 (4)
C(19)	0.4025 (10)	0.1910 (9)	0.0341 (9)	2.8 (3)
C(20)	0.4349 (12)	0.2655 (13)	0.0256 (12)	4.9 (5)
C(21)	0.5219 (14)	0.2854 (16)	0.0610 (15)	7.0 (6)
C(22)	0.5759 (12)	0.2271 (12)	0.1116 (13)	5.3 (5)
C(23)	0.5434 (11)	0.1533 (13)	0.1221 (12)	4.8 (5)
C(24)	0.4568 (11)	0.1347 (11)	0.0838 (10)	3.8 (4)
C(25)	0.2173 (10)	0.2420 (9)	−0.0528 (9)	2.8 (3)
C(26)	0.2344 (10)	0.3000 (12)	−0.1081 (10)	3.8 (4)
C(27)	0.1744 (12)	0.3626 (10)	−0.1373 (11)	4.0 (4)
C(28)	0.0956 (11)	0.3635 (10)	−0.1102 (11)	4.0 (4)
C(29)	0.0756 (10)	0.3069 (10)	−0.0574 (10)	3.3 (4)
C(30)	0.1387 (10)	0.2494 (10)	−0.0290 (9)	3.3 (3)
C(31)	0.3118 (10)	0.1198 (9)	−0.1211 (9)	2.8 (3)
C(32)	0.3946 (11)	0.0895 (12)	−0.1250 (11)	4.2 (4)
C(33)	0.4061 (12)	0.0647 (13)	−0.2049 (12)	5.3 (5)
C(34)	0.3431 (14)	0.0723 (12)	−0.2743 (11)	5.2 (5)
C(35)	0.2637 (15)	0.1014 (12)	−0.2682 (11)	5.0 (5)
C(36)	0.2458 (12)	0.1240 (12)	−0.1931 (11)	4.5 (4)
C(37)	0.3218 (11)	−0.0538 (11)	0.0060 (11)	4.2 (4)
C(38)	0.2183 (11)	−0.0883 (11)	−0.1370 (11)	3.6 (4)
C(39)	0.1319 (10)	0.0107 (9)	−0.0688 (9)	2.7 (3)
C(40)	0.0972 (12)	−0.1493 (12)	0.0450 (15)	7.3 (5)
C(41)	0.0952 (15)	−0.1980 (14)	−0.0413 (13)	9.1 (6)
C(42)	0.1745 (17)	−0.2311 (13)	−0.0311 (15)	8.2 (7)
C(43)	0.2272 (18)	−0.2230 (16)	0.0378 (13)	7.5 (7)
C(44)	0.1866 (15)	−0.1729 (13)	0.0913 (12)	6.4 (6)

[a] Estimated standard deviations in parentheses. [b] *B* values for anisotropically refined atoms are given in the form of the isotropic equivalent thermal parameter defined as $^4/_3[a^2\beta_{11} + b^2\beta_{22} + c^2\beta_{33} + ab(\cos\gamma)\beta_{12} + ac(\cos\beta)\beta_{13} + bc(\cos\alpha)\beta_{23}]$.

Table III. Atomic Coordinates for Non-Hydrogen Atoms and Equivalent Thermal Parameters[a] for $MnPt(\mu\text{-}H)(\mu\text{-}CO)(CO)_4(PEt_3)_2$ (4)

atom[c]	*x*	*y*	*z*	*B*(eqv),[b] Å^2
Pt	0.26554 (4)	0.36952 (3)	0.29495 (4)	2.127 (9)
Mn	0.2279 (2)	0.2832 (1)	0.4696 (2)	2.51 (4)
P(1)	0.3286 (3)	0.3572 (2)	0.1245 (3)	2.52 (6)
C(11A)	0.225 (1)	0.3034 (7)	0.015 (1)	3.2 (3)
C(11B)	0.101 (2)	0.3375 (9)	−0.037 (1)	4.9 (4)
C(12A)	0.477 (1)	0.3106 (8)	0.150 (1)	3.6 (3)
C(12B)	0.578 (2)	0.344 (1)	0.244 (2)	5.2 (4)
C(13A)	0.349 (1)	0.4383 (7)	0.045 (1)	3.4 (3)
C(13B)	0.387 (1)	0.427 (1)	−0.071 (1)	5.5 (4)
P(2)	0.2229 (3)	0.4901 (2)	0.3085 (3)	3.04 (7)
C(21A)	0.335 (1)	0.5538 (7)	0.278 (1)	4.3 (4)
C(21B)	0.466 (2)	0.5399 (9)	0.340 (2)	6.0 (5)
C(22A)	0.078 (1)	0.5152 (8)	0.206 (2)	5.2 (4)
C(22B)	−0.030 (2)	0.478 (1)	0.224 (3)	9.0 (8)
C(23A)	0.207 (1)	0.5162 (8)	0.454 (1)	4.4 (4)
C(23B)	0.173 (2)	0.591 (1)	0.470 (2)	6.9 (6)
C(1)	0.275 (1)	0.2633 (7)	0.317 (1)	2.9 (3)
O(1)	0.3053 (8)	0.2156 (5)	0.2672 (8)	3.3 (2)
C(2)	0.233 (1)	0.1915 (8)	0.504 (1)	3.3 (3)
O(2)	0.239 (1)	0.1319 (5)	0.522 (1)	6.0 (3)
C(3)	0.396 (1)	0.2907 (7)	0.546 (1)	3.5 (3)
O(3)	0.498 (1)	0.2937 (7)	0.594 (1)	6.1 (3)
C(4)	0.187 (1)	0.3224 (8)	0.595 (1)	4.0 (3)
O(4)	0.158 (1)	0.3475 (7)	0.6758 (9)	5.6 (3)
C(5)	0.064 (1)	0.2753 (8)	0.388 (1)	3.9 (3)
O(5)	−0.038 (1)	0.2705 (8)	0.340 (1)	7.2 (4)

[a] Estimated standard deviations in parentheses. [b] *B* values for anisotropically refined atoms are given in the form of the isotropic equivalent thermal parameter defined as $^4/_3[a^2\beta_{11} + b^2\beta_{22} + c^2\beta_{33} + ab(\cos\gamma)\beta_{12} + ac(\cos\beta)\beta_{13} + bc(\cos\alpha)\beta_{23}]$. [c] The B label refers to terminal carbon in ethyl groups.

Table IV. Selected Interatomic Distances (Å) and Angles (deg) with Esd's in $MoPt(H)Cp(CO)_3(PPh_3)_2$ (1)[a]

Bond Distances			
Pt–Mo	2.839 (1)	P(1)–C(1)	1.81 (1)
Pt–P(1)	2.264 (3)	P(1)–C(7)	1.84 (1)
Pt–P(2)	2.355 (3)	P(1)–C(13)	1.82 (1)
Mo–C(37)	1.97 (1)	P(2)–C(19)	1.84 (1)
Mo–C(38)	1.93 (1)	P(2)–C(25)	1.86 (1)
Mo–C(39)	1.95 (1)	P(2)–C(31)	1.85 (1)
Mo–C(40)	2.35 (1)		
Mo–C(41)	2.36 (1)	Pt···C(37)	2.61 (1)
Mo–C(42)	2.37 (2)	Pt···C(39)	2.51 (1)
Mo–C(43)	2.46 (2)	P···H(12)	2.95
Mo–C(44)	2.42 (2)	Pt···H(30)	3.00
C(37)–O(37)	1.16 (2)	Pt···H(24)	3.03
C(38)–O(38)	1.16(2)	Pt···H(14)	3.22
C(39)–O(39)	1.15 (1)		
Bond Angles			
Mo–Pt–P(1)	149.1 (1)	Pt–P(1)–C(1)	120.9 (3)
Mo–Pt–P(2)	108.8 (1)	Pt–P(1)–C(7)	111.1 (3)
P(1)–Pt–P(2)	101.3 (1)	Pt–P(1)–C(13)	115.0 (3)
Pt–Mo–C(37)	62.6 (2)	C(1)–P(1)–C(7)	102.3 (6)
Pt–Mo–C(38)	115.5 (2)	C(1)–P(1)–C(13)	103.4 (6)
Pt–Mo–C(39)	59.9 (2)	C(7)–P(1)–C(13)	101.7 (5)
C(37)–Mo–C(38)	83.2 (6)	Pt–P(2)–C(19)	111.8 (4)
C(37)–Mo–C(39)	104.3 (6)	Pt–P(2)–C(25)	112.8 (4)
C(38)–Mo–C(39)	81.1 (6)	Pt–P(2)–C(31)	119.1 (3)
Mo–C(37)–O(37)	169 (1)	C(19)–P(2)–C(25)	109.1 (6)
Mo–C(38)–O(38)	176 (1)	C(19)–P(2)–C(31)	102.2 (6)
Mo–C(39)–O(39)	168 (1)	C(25)–P(2)–C(31)	100.7 (6)

[a] Numbers in parentheses are estimated standard deviations in the least significant digits.

which were assigned to the ν(PtH) vibrations and which are typical for terminal hydride ligands.[21] This IR absorption is shifted by ca. 112 and 104 cm^{-1}, respectively, when compared with that in *trans*-$PtH(Cl)(PPh_3)_2$ (2220 cm^{-1}).[9] This is explained by the higher trans influence of the phosphine ligand in **1** or **2** compared to Cl in the precursor complex. The ν(CO) frequencies for KBr pellets of **1**, at 1919, 1831, and 1803 cm^{-1}, and of **2**, at 1917, 1828, and 1808 cm^{-1}, correspond to a pattern typical for a $CpM(CO)_3X$ "four-legged piano-stool" structure (see below). Their rather low values are indicative of the metal–metal bond being more polar in these complexes ($Pt^{\delta+}$—$m^{\delta-}$) than, e.g., in the corresponding m–PtL_2–m trinuclear complexes.[7,19,20] In other words, the $[PtH(PPh_3)_2]^+$ fragment acts as a stronger Lewis acid than does $[m\text{-}PtL_2]^+$ toward $[M(CO)_3Cp]^-$. These ν(CO) frequencies are also consistent with carbonyl ligands being semibridging, as indicated by the results of the crystal structure determination of **1** (see below). The ^1H and ^{31}P NMR data

---

(21) Kaesz, H. D.; Saillant, R. B. *Chem. Rev.* **1972**, *72*, 231.

Table V. Selected Interatomic Distances (Å) and Angles (deg) with Esd's in $MnPt(\mu\text{-}H)(\mu\text{-}CO)(CO)_4(PEt_3)_2)$ (4)[a]

Bond Distances			
Pt–Mn	2.730 (2)	P(2)–C(22A)	1.81 (1)
Pt–P(1)	2.283 (3)	P(2)–C(23A)	1.81 (1)
Pt–P(2)	2.353 (3)	C(11A)–C(11B)	1.51 (2)
Pt–C(1)	2.03 (1)	C(12A)–C(12B)	1.49 (2)
Mn–C(1)	2.02 (1)	C(13A)–C(13B)	1.53 (2)
Mn–C(2)	1.79 (1)	C(21A)–C(21B)	1.47 (2)
Mn–C(3)	1.87 (1)	C(22A)–C(22B)	1.47 (2)
Mn–C(4)	1.81 (1)	C(23A)–C(23B)	1.50 (2)
Mn–C(5)	1.84 (1)	C(1)–O(1)	1.17 (1)
P(1)–C(11A)	1.80 (1)	C(2)–O(2)	1.15 (1)
P(1)–C(12A)	1.83 (1)	C(3)–O(3)	1.12 (1)
P(1)–C(13A)	1.85 (1)	C(4)–O(4)	1.17 (1)
P(2)–C(21A)	1.84 (1)	C(5)–O(5)	1.13 (2)
Bond Angles			
Mn–Pt–P(1)	136.7 (1)	C(2)–Mn–C(5)	90.5 (6)
Mn–Pt–P(2)	117.6 (1)	C(3)–Mn–C(4)	90.7 (6)
Mn–Pt–C(1)	47.4 (3)	C(3)–Mn–C(5)	177.5 (5)
P(1)–Pt–P(2)	105.7 (1)	C(4)–Mn–C(5)	91.7 (6)
P(1)–Pt–C(1)	89.4 (3)	C(11A)–P(1)–C(12A)	103.2 (6)
P(2)–Pt–C(1)	164.3 (3)	C(11A)–P(1)–C(13A)	104.7 (5)
Pt–Mn–C(1)	47.9 (3)	C(12A)–P(1)–C(13A)	105.3 (5)
Pt–Mn–C(2)	138.8 (4)	C(21A)–P(2)–C(22A)	103.3 (7)
Pt–Mn–C(3)	89.1 (4)	C(21A)–P(2)–C(23A)	103.4 (6)
Pt–Mn–C(4)	118.5 (4)	C(22A)–P(2)–C(23A)	105.5 (7)
Pt–Mn–C(5)	89.1 (4)	Pt–C(1)–Mn	84.7 (4)
C(1)–Mn–C(2)	90.9 (5)	Pt–C(1)–O(1)	136.0 (9)
C(1)–Mn–C(3)	89.0 (5)	Mn–C(1)–O(1)	138.9 (9)
C(1)–Mn–C(4)	166.4 (5)	Mn–C(2)–O(2)	177 (1)
C(1)–Mn–C(5)	88.5 (5)	Mn–C(3)–O(3)	178 (1)
C(2)–Mn–C(3)	89.7 (6)	Mn–C(4)–O(4)	179 (1)
C(2)–Mn–C(4)	102.7 (5)	Mn–C(5)–O(5)	178 (1)

[a] Numbers in parentheses are estimated standard deviations in the least significant digits.

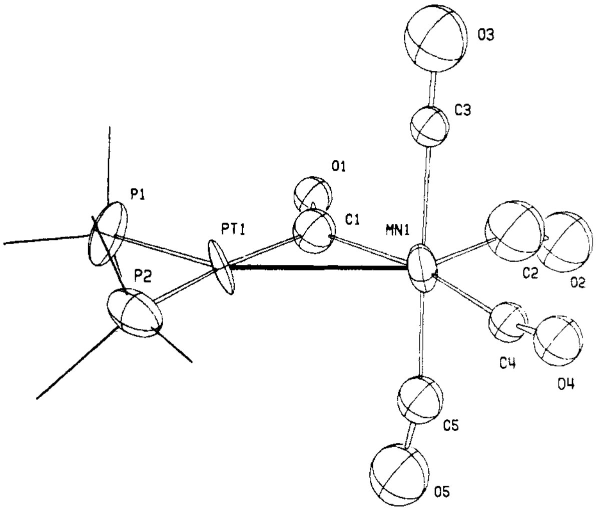

Figure 2. A view of the molecular structure of $MnPt(\mu\text{-}H)(\mu\text{-}CO)(CO)_4(PEt_3)_2$ (4). The bridging hydride is not shown. Ethyl groups were ommitted for clarity. A drawing showing the complete atom numbering scheme is given in the supplementary material.

(see Experimental Section and below) for 1 are consistent with the structure drawn in eq 2.

The reactions in eq 3 were carried out at low temperature in order to avoid decomposition of the thermally sensitive bimetallic products. Solutions and crystals of 3 and 4 are best stored below 0 °C. The IR spectra of these complexes show ν(CO) absorptions typical for terminal carbonyl ligands, between ca. 2050 and 1900 cm^{-1}, and a strong absorption typical for a bridging carbonyl, between 1730 and 1708 cm^{-1}. On the other hand, no IR absorption typical for a terminal metal hydride was observed for 3 or 4, in contrast to that found for 1 and 2. We made no attempt to locate the IR absorption of the bridging hydride as it is well-known that such absorptions are often difficult to assign and are usually weak.[21] Together with the ^1H and $^{31}P\{^1H\}$ NMR data discussed below, these observations were consistent with the structure drawn in eq 3 for 3 and 4 and confirmed by an X-ray diffraction study of 4. This latter complex can be handled for very short periods (ca. 5 min) as a solid in air without decomposition. After longer periods of time, it turns brown and smells of PEt_3.

X-ray Diffraction Study of $MoPt(H)Cp(CO)_3(PPh_3)_2$ (1). The crystal structure consists of discrete molecular units, separated by normal van der Waals distances. A drawing of the molecular structure of complex 1 is shown in Figure 1. Selected bond distances and angles are given in Table IV. In this bimetallic complex, the Mo atom is bonded to three carbonyls, the Cp ligand, and the Pt atom while the Pt atom is further bonded to two PPh_3 ligands and a H ligand. The platinum atom is located in the plane defined by the two phosphorus and the molybdenum atoms (see least-squares planes in Table X of the supplementary material). The square environment usually found for Pt(II) complexes is strongly distorted. The P(1)–Pt–P(2) and P(2)–Pt–Mo angles in 1 are much larger than the normal angle between cis ligands in order to minimize the steric repulsions between the bulky groups, as also found in, e.g., $[PtH(PPh_3)_3][(CF_3CO_2)_2H]$.[22] The value of the third angle, P(1)–Pt–Mo, confirms the planar environment about the Pt atom. Although the hydride ligand H(1) could not be located on the final difference Fourier map, it was confidently placed on the bisectrix of the large P(1)–Pt–Mo angle, leading to a P(2)–Pt–H(1) angle of 183.4 (1)°. For the calculation of H(1) atomic coordinates, a Pt–H(1) distance of 1.6 Å was chosen, which corresponds to the average distance observed for terminal platinum hydrides.[23] The platinum–phosphorus distances are significantly different, as expected form the geometry of the complex. The larger Pt–P distance corresponds to the phosphorus atom trans with respect to the hydrido ligand, of high trans influence.[24] The Mo–Pt distance of 2.839 (1) Å is in the range found for other molybdenum–platinum complexes in which a $Mo(CO)_3Cp$ group in bonded to one or two Pt atoms.[7] The geometry about the Mo atom is of the "four-legged piano stool" type, usual for $CpMo(CO)_3X$ derivatives.[25]

The C(38)O(38) ligand, which is almost in the platinum coordination plane (at –0.10 (2) Å from it), is linear. The carbonyls C(37)O(37) and C(39)O(39) are bent toward the platinum atom, in a semibridging manner,[26] with Mo–C(37)–O(37) and Mo–C(39)–O(39) angles of 169 (1) and 168 (1)° and Pt–C(37) and Pt–C(39) distances of 2.61 (1) and 2.51 (1) Å, respectively. The geometry of the metal carbonyl fragment in 1 bears a stronger ressemblance to that found in, e.g., *trans*-$Pt(RNC)[C(OEt)(NHR)][Mo(CO)_3Cp]_2$ ($R = c\text{-}C_6H_{11}$)[20] than it does to that found in, e.g., $CpMo(CO)_3(HgCl)$[25] which has three linear CO's.

The plane of the cyclopentadienyl ligand of 1 is at 2.060 (1) Å from the molybdenum atom and makes an angle of 89.3 (2)° with the platinum coordination plane. The shortest Pt···H intramolecular contacts within 1 are given in Table IV and are all superior to 2.9 Å. Dimensions within the C_5H_5 and PPh_3 ligands are normal.

X-ray Diffraction Study of $MnPt(\mu\text{-}H)(\mu\text{-}CO)$-

---

(22) Caputo, R. E.; Mak, D. K.; Willet, R. D.; Roundhill, S. G. N.; Roundhill, D. M. *Acta Crystallogr., Sect. B: Struct. Crystallogr. Cryst. Chem.* **1977**, *B33*, 215.

(23) Teller, R. G.; Bau, R. *Struct. Bonding (Berlin)* **1981**, *44*, 1.

(24) Chatt, J. *Proc. Chem. Soc.* **1962**, 318.

(25) Bueno, C.; Churchill, M. R. *Inorg. Chem.* **1981**, *20*, 2197.

(26) Colton, R.; McCormick, M. J. *Coord. Chem. Rev.* **1980**, *31*, 1.

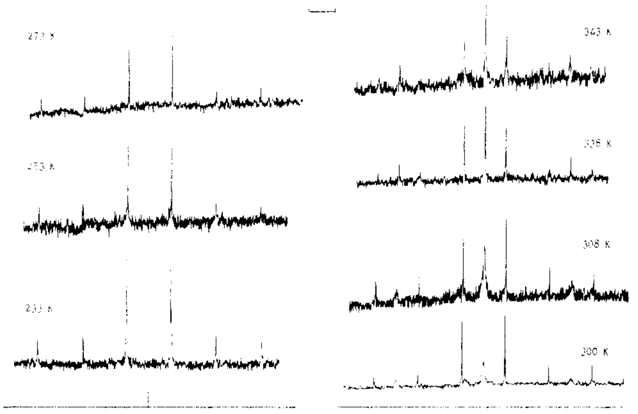

Figure 3. Variable-temperature ^1H NMR spectra for 1 in toluene. The bar represents 100 Hz.

$(CO)_4(PEt_3)_2$ (4). The crystal structure of 4 consists of discrete molecular units, separated by normal van der Waals distances. An ORTEP drawing of 4 is shown in Figure 2. Bond distances and angles are given in Table V. In this complex, the Mn atom is bonded to four terminal carbonyls, the Pt atom is bonded to two PEt_3 ligands, and a bridging carbonyl and a bridging hydride span the metal–metal bond. The hydride ligand was not located although the overall geometry of the molecule and the spectroscopic data are consistent with its bridging the two metals. In this position, the four ligands H, C(1)O(1), and $(PEt_3)_2$ approximate a square-planar geometry about Pt whereas the μ-H and the five CO's give a near-perfect octahedral geometry at Mn (see the interligand angles in Table V). The Pt–P(1) and Pt–P(2) distances are 2.283 (3) and 2.353 (3) Å, respectively.[27] The carbonyl C(1)O(1) is symmetrically bound to Mn and Pt with metal–C(1) distances of 2.02 (1) and 2.03 (1) Å, respectively. The Mn–Pt distance of 2.730 (2) Å is in the range found for this bond in organometallic complexes[28] and is close to the value of 2.738 (1) Å found for the unbridged Mn–Pt bond in $Mn_2Pt(CO)_{12}$.[28] Dimensions within the PEt_3 ligands are normal.

Dynamic Stereochemistry of 1 and 4. Complexes 1–4 in toluene present variable-temperature ^1H NMR spectra indicative of a dynamic behavior. A study was undertaken with pure samples of 1 and 4. The ^1H NMR spectrum of 1 at 233 K shows a doublet at −5.73 ppm for the hydride ligand with ^{195}Pt satellites: $^1J(Pt\text{–}H) = 678$ Hz. The doublet structure originates from coupling with the trans phosphorus P(2) only: $|^2J(P\text{–}H)| = 170$ Hz. The fact that $^2J[P(1)\text{–}H]$ is accidentally equal or close to zero[29] was confirmed by a selective decoupling (phenyl protons) ^{31}P NMR experiment where only P(2) appeared as a doublet with $|^2J(P\text{–}H)| \approx 150$ Hz. Upon warming to room temperature, a central resonance begins to appear in the middle of the doublet of the ^1H NMR spectrum, associated with ^{195}Pt satellites (Figure 3). Upon further warming, the new resonance in the ^1H NMR spectrum continues to gain intensity, and at 343 K, a 1:2:1 triplet pattern is observed. A parallel behavior is observed for the high- and low-field satellites (Figure 3). The measured coupling constant $^2J(PH)$ in the triplet is 80 Hz, corresponding to the average value $^1/_2[|^2J(P(1)H)| + {}^2J(P(2)H)|]$ and confirming that the external lines of the triplet derive from the low-temperature doublet. At 228 K, the $^{31}P\ \{^1H\}$ NMR spectrum of 1 shows the expected AB pattern ($^2J(PP) \approx 6$ Hz) with ^{195}Pt satellites. The resonance with the smaller coupling $^1J(PtP) = 2653$ Hz is assigned to P(2), trans to the hydride ligand, and this is consistent with the selective decoupling experiment (see Experimental Section). At room temperature, the $^{31}P\ \{^1H\}$ NMR spectrum is a singlet at ~34 ppm ($\Delta\nu_{1/2} \approx 15$ Hz), indicating equivalent phosphorus atoms. Cooling the sample regenerates the low-temperature spectra, and these reversible changes with the temperature can be followed for many cycles.

The ^1H NMR spectrum of 4 at 250 K shows a doublet of doublets pattern, centered at −3.80 ppm, with ^{195}Pt satellites. This is consistent with the static structure shown in Figure 2, which indicates two nonequivalent phosphine ligands. The trans-coupling $|^2J(P(1)H)| = 76.7$ Hz is smaller than for 1, whereas the cis-coupling $|^2J(P(2)H)| = 29.2$ Hz is larger. Upon warming, the outer lines of the dd pattern collapse until coalescence occurs around 321 K, while the inner lines remain sharp and at constant separation: $\{|^2J(P(1)H)| - |^2J(P(2)H|\}$. Upon further warming to 341 K, the expected central resonance begins to appear but the full triplet pattern is not yet developed. During this process, the satellite resonances are maintained and follow a comparable change.[6b] The thermal instability of the compound prevents heating to higher temperatures. There is a slight dependence of δ with the temperature since at 293 K, the hydrido resonance is located at δ −4.0. The $^{31}P\ \{^1H\}$ NMR spectrum of 4 at 291 K shows broad resonances ($^2J(PP)$ unresolved, $\Delta_{1/2} \approx 53$ Hz) centered at δ 5.69 and 29.15 with $^1J(PtP)$ coupling constants of 2167 and 4580 Hz for P(2) and P(1), respectively. Both resonances broaden upon allowing the hydride ligand to couple, with the downfield resonance clearly showing $|^2J(PH)| \approx 49$ Hz and therefore assigned to the phosphorus trans to the hydride, while the half-width of the upfield resonance approximately doubles to $\Delta_{1/2} \approx 101$ Hz. At 233 K, these values become 52 and 82 Hz, respectively. Here again, the changes observed in the NMR spectra are reversible when decreasing the temperature.

The dynamic behavior of 1 and 4 is therefore quite similar. It is concentration independent, ruling out a bimolecular exchange process. The retention of spin coupling in the high-temperature ^1H NMR spectrum clearly indicates that the equivalencing of the two phosphine ligands with the temperature is an intramolecular process and it can be rationalized by the following spin diagram:

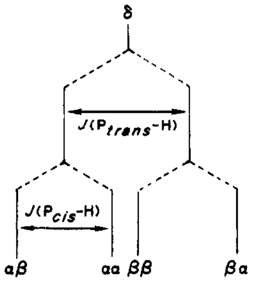

As the temperature is raised, the phosphines exchange positions but to the hydride the $\alpha\alpha$ and $\beta\beta$ spin states appear the same and remain unchanged. However, the $\alpha\beta$ and $\beta\alpha$ spin states average into a single resonance midway between these two. The high-temperature limiting spectrum would reflect the following diagram, as actually observed for complex 1:

---

[27] Russel, D. R.; Mazid, M. A.; Tucker, P. A. *J. Chem. Soc., Dalton Trans.* **1980**, 1737.

[28] Bars, O.; Braunstein, P.; Jud, J. M. *Nouv. J. Chim.* **1984**, *8*, 771.

[29] For a precedent of zero $^2J(P\text{–}H)$ coupling in a cis P–Pt–H arrangement, see, e.g. Green, M.; Mead, K. A.; Mills, R. M.; Salter, I. D.; Stone, F. G. A.; Woodward, P. *J. Chem. Soc., Chem. Commun.* **1982**, 51.

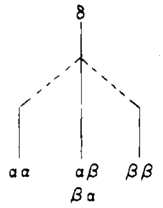

A consequence of the collapse of the outer resonances is that the coupling constants of the hydride to the two phosphorus atoms must be of opposite sign. A similar situation was found for fluxional *cis*-$PtH(SiR_3)(PPh_3)_2$ in which also rapid intramolecular exchange of the PPh_3 ligands occurs.[30]

What is the mechanism for the phosphine exchange? The data indicate the exchange to be intramolecular, and thus dissociation of a molecular fragment completely beyond the solvent cage cannot be occurring. However, the NMR data do not distinguish a purely intramolecular nondissociative process from one where temporary dissociation, molecular rotation, and recombination occur without solvent-cage escape. This ambiguity has been previously discussed for the observed fluxionality of *cis*-$PtH(SiR_3)(PPh_3)_2$[30] and $MnH(SiPh_3)Cp(CO)_2$.[31] From detailed variable-temperature NMR investigations on $[NiP_3H]^+$ systems, it was also concluded that their rearrangement is exclusively intramolecular in nature, although its detailed mechanism is not known.[32] The various fluxional possibilities for our complexes are presented in the Discussion.

Chemical Behavior of the Mo-Pt, W-Pt, and Mn-Pt Complexes. During the synthesis of complex 1, we observed that the reaction mixture was best kept at low temperature, resulting in higher yields of 1 (see Experimental Section). When thermal decomposition of the solution occurred under N_2, two platinum clusters were found in small quantities: $Pt_4(\mu\text{-}CO)_5(PPh_3)_4$[12] and $Pt_5(\mu\text{-}CO)_5(CO)(PPh_3)_4$.[13] They were identified by analytical methods and comparison with authentic samples. We have not identified the molybdenum-containing species. Coordinatively unsaturated Pt(0) fragments, e.g., PtL_2, could form aggregate, coordinate CO molecules, and lead to the stable clusters observed. When separation of 1 from the reaction mixture was attempted by column chromatography under N_2 on silica gel (see Experimental Section), rapid decomposition was observed. Thus, $[Mo(CO)_3Cp]_2$, $Pt_5(\mu\text{-}CO)_5(CO)(PPh_3)_4$,[13] *trans*-$PtH(Cl)(PPh_3)_2$, $Pt_2Mo_2Cp_2(CO)_6(PPh_3)_2$,[7] and $Pt(PPh_3)_3$ were successively eluted with pentane/toluene. A blank chromatographic experiment starting from *pure* 1 led to analogous results: migration of 1 on a silica gel column results very rapidly in its fragmentation. Phosphine labilization and/or oxidation by the inorganic support, accounting for the PPh_3:Pt ratio observed in the products, would generate unsaturated platinum fragments and lead eventually to cluster complexes. The origin of the $PtH(Cl)(PPh_3)_2$ isolated after chromatography was not due to unreacted starting material, because of both the Pt:Mo stoichiometry used and the reproducibility of this observation. Interestingly, we had also found this hydride complex after the chromatographic separation of the products resulting from the reaction between $PtCl_2(PPh_3)_2$ and 2 equiv of $Na[Mo(CO)_3Cp]$.[7] We therefore suggest that some unsaturated Pt-containing fragments generated during chromatography will capture a hydrogen ligand from the residual water on the support (or less likely from the solvent or from an organic ligand). The chloride ligand can only originate from the NaCl dissolved in the reaction mixture and therefore not totally removed by the filtration done before chromatography.

Scheme I

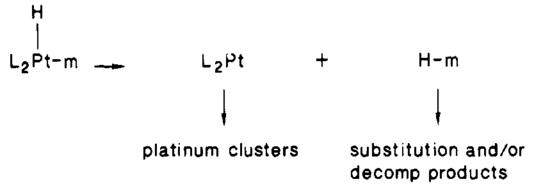

L = PR_3; m = $Mo(CO)_3Cp$, $W(CO)_3Cp$, $Mn(CO)_5$

Solutions of complex 2 slowly decomposed, and the platinum cluster $Pt_4(\mu\text{-}CO)_5(PPh_3)_4$[12] was again isolated by fractional crystallization from toluene. Chromatographic isolation of 2 also failed, and it is noteworthy that the only platinum cluster isolated under these conditions was $Pt_5(\mu\text{-}CO)_5(CO)(PPh_3)_4$,[13] likely formed from the chromatographic transformation of lower nuclearity platinum cluster(s).[33]

When the reaction mixture containing 3 was stirred at room temperature, only homonuclear species could be characterized. They were isolated by fractional crystallization: black $Pt_4(\mu\text{-}CO)_5(PPh_3)_4$,[12] yellow $Pt_2Cl_2(\mu\text{-}CO)(PPh_3)_3$,[14] red $Pt_3(\mu\text{-}CO)_3(PPh_3)_4$,[12] $Mn_2(CO)_{10}$, $Mn_2(CO)_9PPh_3$ and $Mn_2(CO)_8(PPh_3)_2$.[15] These were identified by comparison with authentic samples whereas other products present could not be identified.

The thermal decomposition of 4 was followed in freshly distilled THF solution. Heating at 60 °C induces disappearance of the characteristic IR bands of 4, and new bands grow in at 2050 (w), 1950 (vs), 1940 (m, sh), 1923 (m), 1893 (w), 1860 (w), and 1772 (m) cm^{-1}. These spectral changes appear clean and imply the formation of few products only. The ^1H NMR spectrum of a sample that had been heated to 60 °C for 2 h and let stand at room temperature for 1 week showed only one hydride resonance at δ -7.88 (d, 1 H, $J(PH)$ = 36.7 Hz) with no ^{195}Pt satellites, implying that the hydrogen was attached to Mn and not Pt. This solution was evaporated and extracted with pentane and the IR recorded. It was basically similar to that obtained after heating in THF, except that the resolution was far superior (2058 (m), 1980 (s), 1961 (vs), 1950 (vs), 1780 (m) cm^{-1}). The ^1H NMR and IR data are consistent with the formation of $HMn(CO)_4PEt_3$ (lit. data:[34] IR ν(CO) (cyclohexane) 2060 (vs), 1985 (vs), 1970 (vs), 1960 (vs), 1940 (vw) cm^{-1}; ^1H NMR δ -6.43, $J(PH)$ = 34 Hz; ^1H NMR[35] δ -7.65 ($J(PH)$ = 36 Hz)). It clearly appears that the hydride is transferred from Pt to Mn. The IR absorption below 1800 cm^{-1} is most likely due to a Pt_3 or Pt_4 carbonyl cluster(s).[12]

Therefore, the reaction shown in Scheme I appears to be a general pathway for the decomposition of hydrido bimetallic complexes of the type described in this work. It is interesting to relate this scheme to the dynamic behavior of these bimetallic complexes, discussed below.

Discussion

The objectives of this study were twofold. First, we

---

[30] Azizian, H.; Dixon, K. R.; Eaborn, C.; Pidcock, A.; Shuaib, N. M.; Vinaixa, J. *J. Chem. Soc., Chem. Commun.* **1982**, 1020.

[31] Colomer, E.; Corriu, R. J. P.; Marzin, C.; Vioux, A. *Inorg. Chem.* **1982**, *21*, 368.

[32] Eaton, D. R.; McGlinchey, M. J.; Moffat, K. A.; Buist, R. J. *J. Am. Chem. Soc.* **1984**, *106*, 8110.

[33] Bender, R.; Braunstein, P. *J. Chem. Soc., Chem. Commun.* **1983**, 334 and unpublished results.

[34] Whitesides, G. M.; Maglio, G. *J. Am. Chem. Soc.* **1969**, *91*, 4980.

[35] Behrens, H.; Lampe, R. J.; Merbach, P.; Moll, M. *J. Organomet. Chem.* **1978**, *159*, 201.

wanted to investigate the synthesis and properties of new heteropolymetallic hydrido–carbonyl complexes with the idea that the different nature of the metals might manifest itself by selective M–H and/or M–CO interactions involving one or two metal centers.[2] This, in turn, was expected to influence the reactivity of these ligands when compared to that in their mononuclear precursors. The heterobinuclear M–Pt complexes **1**–**4** were prepared by the reaction of *trans*-$\mathrm{PtH(Cl)(PR_3)_2}$ with the corresponding carbonylmetalates and show the presence of a metal–metal bond, a hydride, and carbonyl ligands.

The second objective of this study was to extend our understanding of the details of the reaction of halogeno square-planar transition-metal d^8 complexes with carbonylmetalates $[\mathrm{m}^-]$. Thus, we have shown previously that this general reaction provides an excellent entry into the synthesis of palladium and platinum mixed-metal clusters.[7,10,18–20,36–38] It was also shown in these studies that the nature of two-electron donors L in the $\mathrm{MCl_2L_2}$ (M = Pd, Pt) precursors is of considerable importance in determining the type and the structure of the products formed in such a reaction (Scheme II). The products resulting from a "simple" chloride substitution are only isolated with certain types of ligands L (Scheme IIa). These have in common a small steric bulk. In contrast, with more bulky tertiary phosphines homo- or heteropolynuclear clusters are obtained (Scheme IIb), in which only one $\mathrm{PR_3}$ liand is generally found per M atom. Phosphine lability plays therefore a determining role. For these reasons, it was interesting to determine which route the reaction of *trans*-$\mathrm{PtH(Cl)(PR_3)_2}$ with carbonylmetalates would follow. Phosphine lability could again lead to cluster complexes, or, because of the presence of both only one leaving chloride and the small hydride ligand, phosphine ligands could remain coordinated to platinum, leading to a heterobinuclear complex. The latter pathway applies to this reaction, as shown in eq 2 and 3. This result emphasizes the importance of steric effects in the reactions of halogeno metal complexes with carbonylmetalates.

Scheme II

(a) $\mathrm{MCl_2L_2 + 2Na[m] \rightarrow m\text{-}ML_2\text{-}m + 2NaCl}$

L = Py, RNC, RCN

(b) $\mathrm{MCl_2L_2 + 2Na[m]} \rightarrow$ homo- or heteropolynuclear clusters

$\mathrm{L = PR_3}$

In the metal–metal bonded complexes **1**–**4**, a Pt–H interaction is clearly evidenced by ^{1}H NMR spectroscopy. The overall geometries of complexes **1** and **4** are consistent with the hydride being terminally bound to Pt in **1** and **2** and bridging the Mn–Pt bond in **3** and **4**. This is also supported by the presence of a typical ν(Pt–H terminal) vibration above 2100 $\mathrm{cm^{-1}}$ in the IR spectrum of **1** and **2**, which is not present in the spectrum of **3** or **4**. Furthermore, the value of the ^1J(Pt–H) coupling constant is larger in **1** (678 Hz) than in **4** (409 Hz), consistent with a stronger Pt–H interaction in the former case. The $^{31}\mathrm{P}\{^1\mathrm{H}\}$ NMR data are also consistent with the solid-state structures of **1** and **4**, showing ^2J(PP) values typical for a mutual cis orientation of the $\mathrm{PR_3}$ ligands and ^1J(Pt–P) values typical for such $\mathrm{PR_3}$ ligands bonded to Pt(II).[39] A planar geometry about the Pt atom is found in the structures of **1** and **4**. Whereas the carbonyl ligands in **1** and **2** are terminal or semibridging, only four carbonyls are terminally bound to Mn in **3** or **4**. The fifth, C(1)O(1), spans the Mn–Pt bond and has a typical low IR absorption. Therefore, the geometry about the Mo atom in **1** is the "four-legged piano stool" type and that about the Mn atom in **4** is octahedral. These are the normally preferred coordination geometries for CpMo and Mn carbonyl complexes, and thus the overall geometries of the binuclear complexes are dictated by the coordination preferences of the individual metals. The geometry of the $\overline{\mathrm{Pt}-(\mu\text{-CO})-\mathrm{Mn}}\mathrm{(CO)_4}$ system is interestingly related to that of $\overline{\mathrm{Pt}-(\mu\text{-PPh_2})-\mathrm{Mn}}\mathrm{(CO)_4}$ moieties.[37] In $\mathrm{Mn_2Pt(\mu\text{-}PPh_2)_3H(CO)_8}$, for example

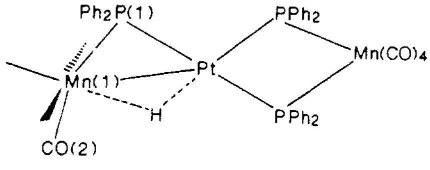

the hydride ligand bonded to platinum was assigned a terminal position on Pt on the basis of its ^{1}H NMR signal at δ −11.1 with ^1J(PtH) = 526 Hz. As the data for **4** indicate, this ^1J(PtH) value, together with the geometry of the $\mathrm{Mn(CO)_4PPh_2}$ fragment, could also be in accord with a bridging hydride, being probably closer to Pt than to Mn. The P(1)–Mn(1)–C(2) angle of 164.3 (5)° in the $\mathrm{Mn_2Pt}$ complex[37] compares with the corresponding C(1)–Mn–C(4) angle of 166.4 (5)° in **4**.

Complexes **1**–**4** follow decomposition pathways in solution or on inorganic supports consistent with reductive elimination of H–m from the complex. Note that reductive elimination of $\mathrm{CH_4}$ also explains the lability of *cis*-$\mathrm{PtH(CH_3)(PPh_3)_2}$.[40] No H to CO transfer was evidenced in our systems and no formation of, e.g.

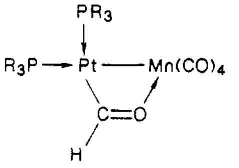

was detected.

Complexes **1**–**4** present an interesting stereodynamic behavior which has been investigated only for the more stable **1** and **4**. Their variable-temperature ^{1}H NMR spectra imply a mutual exchange process that maintains spin correlation and which must be strictly intramolecular. Thorn and Hoffmann[41a] have shown that the potential surface for the rearrangement of $[\mathrm{HPt(PH_3)_2}]^+$ reveals minima for structures **a** and **c** with a very low interconversion barrier, via the "Y" structure **b**. Three-coordinate

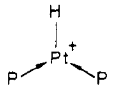

a

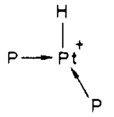

b

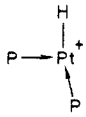

c

platinum(II) moieties are Jahn–Teller systems which prefer

---

[36] Barbier, J. P.; Braunstein, P.; Fischer, J.; Ricard, L. *Inorg. Chim. Acta* **1978**, *31*, L361.

[37] Braunstein, P.; Matt, D.; Bars, O.; Louër, M.; Grandjean, D.; Fischer, J.; Mitschler, A. *J. Organomet. Chem.* **1981**, *213*, 79.

[38] Braunstein, P. *Nouv. J. Chim.* **1986**, *10*, 365.

[39] Pregosin, P. S.; Kunz, R. W. *^{31}P and ^{13}C NMR of Transition Metal Phosphine Complexes*, Springer-Verlag: Berlin, Heidelberg, 1979.

[40] Abis, L.; Sen, A.; Halpern, J. *J. Am. Chem. Soc.* **1978**, *100*, 2915.

[41] (a) Thorn, D. L.; Hoffmann, R. *J. Am. Chem. Soc.* **1978**, *100*, 2079. (b) The NMR spectra support the involvement of only diamagnetic species. We therefore rule out an intermediate of D_{3h} symmetry since in a trigonal-planar structure, the d orbitals of platinum will split in the order $d_{xz}, d_{yz} < d_{z^2} < d_{xy}, d_{x^2-y^2}$, giving rise to two unpaired 5d electrons. See also: Yared, Y. W.; Miles, S. L.; Bau, R.; Reed, C. A. *J. Am. Chem. Soc.* **1977**, *99*, 7076.

T- or Y-shaped C_{2v} structures, avoiding the most symmetrical D_{3h} trigonal geometry. Reasonable explanations for the dynamic behavior of our complexes include[41b] (a) rotation via transient formation within the solvent cage of the dissociated molecular pairs [$(Ph_3P)_2Pt{\cdot}HMo(CO)_3Cp$] or [$(Et_3P)_2Pt{\cdot}HMn(CO)_5$], respectively

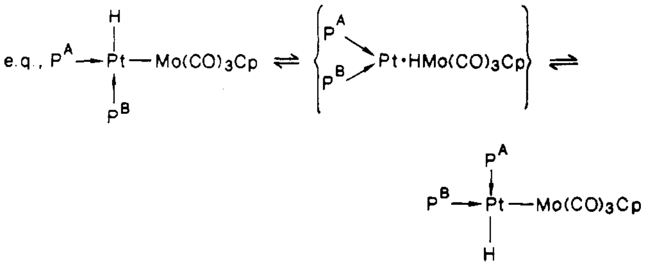

(b) or, less likely, involvment of the molecular pairs [Ph_3P-$(Ph_3P)Pt(H)Mo(CO)_3CP$] or [Et_3P-$(Et_3P)Pt(\mu$-$H)(\mu$-$CO)Mn(CO)_4$], respectively

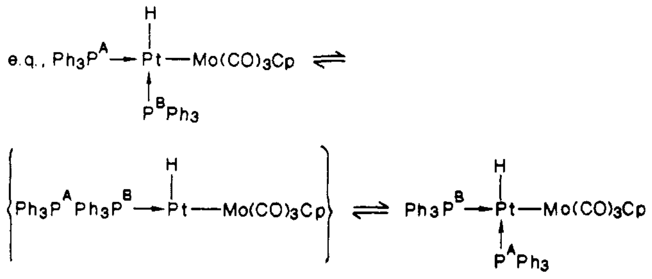

(c) rotation of the C_{2v} d^8 [$HPt(PR_3)_2$]$^+$ fragment within the solvent cage of the dissociated ion pairs {[$HPt(PPh_3)_2$]$^+$[$Mo(CO)_3Cp$]$^-$} or {[$HPt(PEt_3)_2$]$^+$[$Mn(CO)_5$]$^-$}; (d) formation of CO-bridged intermediates, suggested for 4 by the presence of a bridging carbonyl in the ground-state structure, such as $(Et_3P)_2Pt{\cdots}CO{\cdots}MnH(CO)_4$, which however would appear less likely in the case of 1; (e) formation of hydride-bridged intermediates, such as [$(Ph_3P)_2Pt{\cdots}H{\cdots}Mo(CO)_3Cp$] or [$(Et_3P)_2Pt{\cdots}H{\cdots}Mn(CO)_5$], where T- or Y-shaped structure would be involved in the dynamic process[41b]

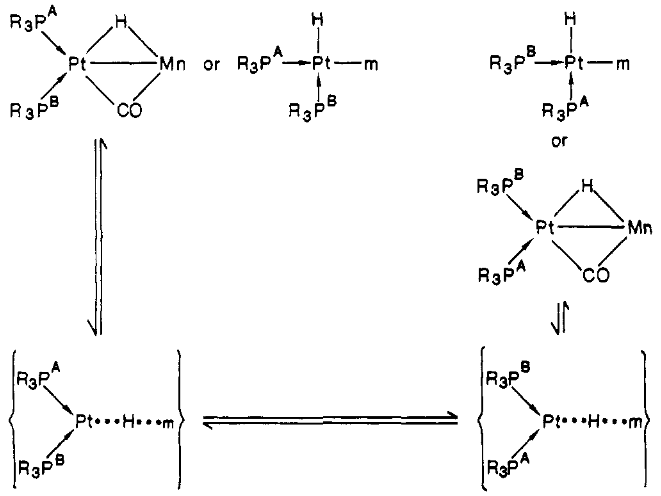

(f) rotation about an axis through the midpoint of the Mo–H and the Mn–H bond as an alternative explanation

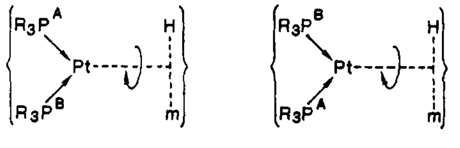

The involvement of the $Pt(PR_3)_2$ and Hm (m = $Mo(CO)_3Cp$, $Mn(CO)_5$) units (via (a), (e), or (f)) appears to us the most interesting possibility since they are reasonable chemical species which could also, after solvent-cage escape, account for the decomposition of the complexes (Scheme I).

Complex 1 has been independently prepared by the reaction of a d^{10} $Pt(PR_3)_2$ fragment with $HMo(CO)_3Cp$,[42] supporting our hypothesis[6b] and showing the reversibility of the reaction of eq 4.

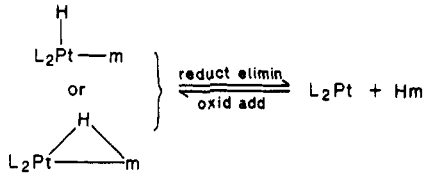

(4)

At this point, it is interesting to recall that oxidative addition of triorganosilanes $SiHR_3$ to the platinum(0) species [$Pt(C_2H_4)L_2$] and [$Pt(C_2H_4)_2L$] affords the complexes *cis*-$PtH(SiR_3)L_2$[43] and [{$Pt(\mu$-$H)(SiR_3)L$}$_2$],[44] respectively, and that oxidative addition of dihydrido–platinum complexes to platinum(0) species has been invoked as an elementary step, followed by protonation, in the synthesis of trihydrido–diplatinum complexes, according to eq 5[45] (cf. the oxidative addition reaction of eq 4).

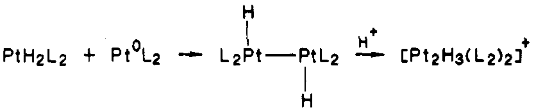

$$PtH_2L_2 + Pt^0L_2 \rightarrow L_2\overset{H}{Pt}\text{—}\underset{H}{Pt}L_2 \xrightarrow{H^+} [Pt_2H_3(L_2)_2]^+ \qquad (5)$$

Interestingly, dissociation of $SiHPh_3$ from $Cp(CO)_2MnH(SiPh_3)$ was invoked to explain its fluxional behavior,[31] a suggestion that has recently received strong support from a neutron diffraction study of the related $(\eta^5$-$CH_3C_5H_4)(CO)_2MnH(SiFPh_2)$ complex, which clearly showed a significant SiH interaction in the ground state of the molecule[46] akin to the bridging hydride in 4. Furthermore, polynuclear platinum-containing complexes have been found to undergo an intramolecular dynamic behavior, although different from that reported here, e.g., *cis*-$Pt(PPh_3)_2(HgGePh_3)(GePh_3)$,[47] $PtW(\mu$-$H)(\mu$-$CHR)(CO)_2(PMe_3)_2Cp$,[48] and [$PtRh_2(\mu$-$H)(\mu$-$CO)_2(CO)(PPh_3)(\eta$-$C_5Me_5)$][BF_4] in which the $Pt(H)(CO)(PPh_3)$ moiety retains its integrity at all times while rotation of the $Rh_2(\mu$-$CO)_2(\eta$-$C_5Me_5)_2$ fragment occurs about an axis through Pt and the midpoint of the Rh=Rh unit.[49] The three-coordinate intermediate $PtH(Ph)(PEt_3)$ has been considered in the isomerization of [$(PEt_3)PhPt(\mu$-$H)_2IrH(PEt_3)_3$]$^+$.[50] Finally, isomerization of the tetrahedral $Os_3Pt(\mu$-$H)_2(\mu$-$CH_2)(CO)_{10}(PCy_3)$ cluster has been de-

---

[42] Researchers at Du Pont, Central Research and Development Department, Wilmington, DE, have carried out this work, together with a calculation of the thermodynamic parameters for the dynamic process reported here. This aspect has therefore not been considered in our work, in order to avoid duplication. Ittel, S. D.; Roe, D. C.; Janowicz, A. H.; Bryndza, H. E., private communication, December 1984.

[43] Eaborn, C.; Ratcliff, B.; Pidcock, A. *J. Organomet. Chem.* **1974**, *65*, 181.

[44] Ciriano, M.; Green, M.; Howard, J. A. K.; Proud, J., Spencer, J. L.; Stone, F. G. A.; Tsipis, C. A. *J. Chem. Soc., Dalton Trans.* **1978**, 801.

[45] Knobler, C. B.; Kaesz, H. D.; Minghetti, G.; Bandini, A. L.; Banditelli, G.; Bonati, F. *Inorg. Chem.* **1983**, *22*, 2324.

[46] (a) Schubert, U.; Ackermann, K.; Wörle, B. *J. Am. Chem. Soc.* **1982**, *104*, 7378. (b) See also: Schubert, U.; Scholz, G.; Müller, J.; Ackermann, K.; Wörle, B.; Stansfield, R. F. D. *J. Organomet. Chem.* **1986**, *306*, 303.

[47] Grishin, Yu. K.; Rosnyatovsky, V. A.; Ustynyuk, Yu. A.; Titova, S. N.; Domrachev, G. A.; Razuvaev, G. A. *Polyhedron* **1983**, *9*, 895.

[48] Jeffery, J. C.; Moore, I.; Stone, F. G. A. *J. Chem. Soc., Dalton Trans.* **1984**, 1571.

[49] Green, M.; Mills, R. M.; Pain, G. N.; Stone, F. G. A.; Woodward, P. *J. Chem. Soc. Dalton Trans* **1982**, 1321.

[50] Boron, P.; Musco, A.; Venanzi, L. M. *Inorg. Chem.* **1982**, *21*, 4192.

scribed as occurring by rotation of the $Pt(CO)(PCy_3)$ fragment about an axis perpendicular to the Os_3 plane.[51]

The chemistry of heteronuclear bridging hydrides is currently actively investigated, from a synthetic, structural, and catalytic point of view.[4,52] The dynamic behavior and the reactivity of the heterobimetallic complexes reported here show their versatility and the potential of this class of complexes. Binuclear systems of the type

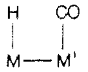

$$\overset{\displaystyle H}{\overset{|}{M}}—\overset{\displaystyle CO}{\overset{|}{M'}}$$

deserve theoretical and further experimental studies. In the systems reported here, migration of the hydride ligand bonded to platinum occurs toward the adjacent metal rather than toward a carbonyl ligand.

Acknowledgment. This work was supported by the Centre National de la Recherche Scientifique (GRECO CO). We are grateful to the Université de Rennes for 1-year leave of absence to O.B. (1980) and to the CNRS for a 6-month temporary appointment (1982/1983) to G.L.G., in the Laboratoire de Chimie de Coordination. We are grateful to Mrs. Kremp and Dr. M. Pfeffer for their assistance in obtaining the NMR spectra. The crystal structure of complex 4 was determined in the Laboratoire de Cristallographie Biologique, IBMC du CNRS, Strasbourg, thanks to the hospitality of Dr. D. Moras. We thank the reviewers for their valuable comments.

Registry No. **1**, 81423-60-1; **2**, 104033-91-2; **3**, 104051-35-6; **4**, 98063-33-3; $Na[Mo(CO)_3Cp]\cdot 2DMF$, 104033-92-3; *trans*-$PtH(Cl)(PPh_3)_2$, 16841-99-9; $Na[W(CO)_3Cp]\cdot 2DMF$, 104033-93-4; $Na[Mn(CO)_5]$, 13859-41-1; *trans*-$PtH(Cl)(PEt_3)_2$, 16842-17-4; $Pt_4(\mu\text{-}CO)_5(PPh_3)_4$, 27518-14-5; $Pt_2Cl_2(\mu\text{-}CO)PPh_3)_3$, 89742-11-0; $Pt_3(\mu\text{-}CO)_3(PPh_3)_4$, 16222-02-9; $Pt_5(\mu\text{-}CO)_5(CO)(PPh_3)_4$, 68875-50-3; $[Mo(CO)_3Cp]_2$, 12091-64-4; $Pt_2Mo_2Cp_2(CO)_6(PPh_3)_2$, 93084-57-2.

Supplementary Material Available: Calculated hydrogen atom positions for 1 and 4 (Tables VI and VII), anisotropic thermal parameters for 1 and 4 (Tables VIII and IX), and selected least-squares planes for 1 and 4 (Tables X and XI) and views of the structures of 1 and 4 with the complete atom labeling scheme (Figures 4 and 5) (12 pages); tables of observed and calculated structure factors for 1 and 4 (Tables XII and XIII) (33 pages). Ordering information is given on any current masthead page.

---

[51] Green, M.; Hankey, D. R.; Murray, M.; Orpen, A. G.; Stone, F. G. A. *J. Chem. Soc., Chem. Commun.* **1981**, 689.

[52] See, for example: (a) Venanzi, L. M. *Coord. Chem. Rev.* **1982**, *43*, 251. (b) Moore, D. S.; Robinson, S. D. *Chem. Soc. Rev.* **1983**, *12*, 415. (c) Arndt, L. W.; Delord, T.; Darensbourg, M. Y. *J. Am. Chem. Soc.* **1984**, *106*, 456. (d) Tooley, P. A.; Arndt, L. W.; Darensbourg, M. Y. *J. Am. Chem. Soc.* **1985**, *107*, 2422.

Preparation, Properties, and Reactions of Metal-Containing Heterocycles. 51.[1] Three- and Five-Membered Phosphacobaltacycloalkanes

Ekkehard Lindner,* Petra Neese, Wolfgang Hiller, and Riad Fawzi

Institut für Anorganische Chemie der Universität, Auf der Morgenstelle 18, D-7400 Tübingen 1, West Germany

Received January 30, 1986

The synthesis of three- and five-membered phosphacobaltacycloalkanes $(OC)_3\overline{CoPPh_2CH_2}$ (**3a**), $(OC)_3\overline{CoPPh_2(CH_2)_3}$ (**4a**), and $(OC)_3\overline{CoP(C_6H_{11})_2(CH_2)_3}$ (**4b**) by reductive cycloelimination of $[(OC)_3CoPPh_2CH_2Cl]_2$ (**1a**), $[(OC)_3CoPPh_2(CH_2)_3Cl]_2$ (**2a**), and $[(OC)_3CoP(C_6H_{11})_2(CH_2)_3Cl]_2$ (**2b**) is described. Reaction of the five-membered ring with CO or PPh_3 results either in CO insertion into the metal–alkyl C bond forming $(OC)_3\overline{CoPPh_2(CH_2)_3C}{=}O$ (**5a**), $(OC)_3\overline{CoP(C_6H_{11})_2(CH_2)_3C}{=}O$ (**5b**), and $Ph_3P(OC)_2\overline{CoPPh_2(CH_2)_3C}{=}O$ (**6a**), respectively, or in CO substitution yielding $Ph_3P(OC)_2\overline{CoP(C_6H_{11})_2(CH_2)_3}$ (**7b**). The products were characterized by IR, NMR (^1H, ^{13}C, and ^{31}P), and mass spectroscopy. Single crystals of $(OC)_3\overline{CoPPh_2CH_2}$ (**3a**) are monoclinic of space group $P2_1/c$ with a = 10.498 (4) Å, b = 7.697 (3) Å, c = 18.783 (5) Å, β = 98.29 (2)°, and Z = 4. Single crystals of $(OC)_3\overline{CoP(C_6H_{11})_2(CH_2)_3}$ (**4b**) are triclinic of space group $P\bar{1}$ with a = 9.999 (5) Å, b = 12.910 (5) Å, c = 8.364 (3) Å, α = 101.81 (3)°, β = 101.28 (3)° γ = 112.44 (4)°, and Z = 2. The cobalt coordination in $(OC)_3\overline{CoPPh_2CH_2}$ (**3a**) is a distorted trigonal bipyramid. According to a short P–C(4) bond of 1.725 (5) Å the $\overline{Co\text{–}P\text{–}C}$ ring is described as a phosphorus ylide with a complexed ylidic C(4) atom. $(OC)_3\overline{CoP(C_6H_{11})_2(CH_2)_3}$ (**4b**) is essentially a metallacyclopentane with a trigonal-bipyramidal coordinated cobalt.

Introduction

Interest in metallacycloalkanes recently increased due to their presumed role in transition-metal-catalyzed reactions.[2] This is also true for complexes with donor atoms in the metallacycle.[3,4] Cobalt is of increasing importance as a component of highly reactive catalytic systems.[5] Continuing earlier studies of three- to seven-membered

---

[1] Part 50: Lindner, E.; Fawzi, R. *J. Organomet. Chem.* **1986**, *299*, C47.

[2] (a) Lindner, E. *Adv. Heterocycl. Chem.* **1986**, *39*, 237. (b) Puddephatt, R. J. *Comments Inorg. Chem.* **1982**, *2*, 69. (c) Lindner, E.; Schauss, E.; Hiller, W.; Fawzi, R. *Chem. Ber.* **1985**, *118*, 3915. (d) Stockis, A.; Hoffmann, R. *J. Am. Chem. Soc.* **1980**, *102*, 2952. (e) McKinney, R. J.; Thorn, D. L.; Hoffmann, R.; Stockis, A. *J. Am. Chem. Soc.* **1981**, *103*, 2595.

[3] Roberto, D.; Alper, H. *Organometallics* **1984**, *3*, 1767.

[4] (a) Lindner, E.; Zinsser, F.; Hiller, W.; Fawzi, R. *J. Organomet. Chem.* **1985**, *288*, 317. (b) Lindner, E.; Funk, G.; Hoehne, S. *Chem. Ber.* **1981**, *114*, 3855. (c) Lindner, E.; Funk, G.; Hoehne, S. *J. Organomet. Chem.* **1981**, *214*, C7.

[5] (a) Ugo, R. In *Catalysis by Metal Complexes, Catalysis in C_1 Chemistry*; Keim, W., Ed.; D. Reidel Publishing: Dordrecht, Boston, Lancaster, 1983; p 135. (b) Costa, L. C. *Catal. Rev.—Sci. Eng.* **1983**, *25*, 325.

0276-7333/86/2305-2030$01.50/0 © 1986 American Chemical Society